GAS HYDRATE ASSESSMENT USING A MARINE BOTTOM-TOWED CONTROLLED SOURCE ELECTROMAGNETIC SYSTEM: LATEST RESULTS FROM CASCADIA

Katrin Schwalenberg
Federal Institute for Geosciences and Natural Resources, Stilleweg 2, 30655 Hannover, Germany, Phone: + 49 511 643 2718, Fax: +49 511 643 3663,
Email: k.schwalenberg@bgr.de

Carsten Scholl, Reza Mir, R. Nigel Edwards
University of Toronto, Department of Physics, 60 St. George St., Toronto M5S 1A7, Canada

Ele C. Willoughby
Pacific Geoscience Centre, Geological Survey of Canada,9860 West Saanich Road, P.O. Box 6000, Sidney, B.C. V8L 4B2, Canada

Introduction

CSEM data collected along four profiles over a cold vent field in an area characterized by expanded gas hydrate deposits on the Cascadia Margin, Western Canada, show highly anomalous resistivity anomalies over the vents. The resistivities are more than 4 times higher than the regional background.

Submarine gas hydrates have been identified along the Cascadia Margin in many seismic data through the occurrence of bottom simulating reflectors (BSRs) and during the Ocean Drilling Program (ODP Leg 146). Hydrate deposits occur over large portions along the slope (e.g. Spence et al., 2000). A series of seismic blank zones was found in different seismic data sets in a cold vent field (Riedel et al., 2002). The vent field is located on a bathymetric bench in approximately 1300m water depth close to ODP site 889 and consists of at least 4 vents with diameters from 80m to 400m in an area of roughly 1km x 3km (Figure 1). Massive hydrate samples have been recovered from piston cores just below the seafloor at “Bullseye” which is the largest of the vents (Riedel et al., 2002). Bullseye is also one of four drill sites along a transect crossing the Cascadia Margin which was completed in fall 2005 within the Integrated Ocean Drilling Program (IODP Leg 311, Expedition 311 Scientists, Prelim Rep. 2005).
The causes of venting at Bullseye have been diversely discussed, taking mainly seismic data, seafloor observation and core data into account (see review by Riedel et al., 2006). Alternative methods like compliance (Willoughby et al., 2005) and controlled source electromagnetics (CSEM) (Schwalenberg et al., 2005) operate on a different scale. Compliance data are particularly sensitive to the shear modulus and therefore to the strength of the seafloor sediments. The electrical conductivity derived from CSEM data is mainly controlled by the amount of interstitial seawater and is therefore a function of the porosity and subsequently of the salinity and temperature of the seawater. Regionally, the conductivity or its reciprocal, the resistivity, is in the order of 1-2 Ωm for the upper 100 mbsf.

Gas hydrate forms within the temperature and pressure controlled gas hydrate stability zone (GHSZ) where it replaces conductive pore fluid. Subsequently the bulk resistivity of the seafloor is enhanced if gas hydrate is present in sufficient quantities. Gas hydrate concentrations can be estimated from the empirical relation known as Archie’s law (Archie, 1942). It is

$$\rho_f = a\rho_\omega \Phi^{-m}$$

for a simple two-phase system, or

$$\rho_f = a\rho_\omega \Phi^{-m} S_\omega^{-n}$$

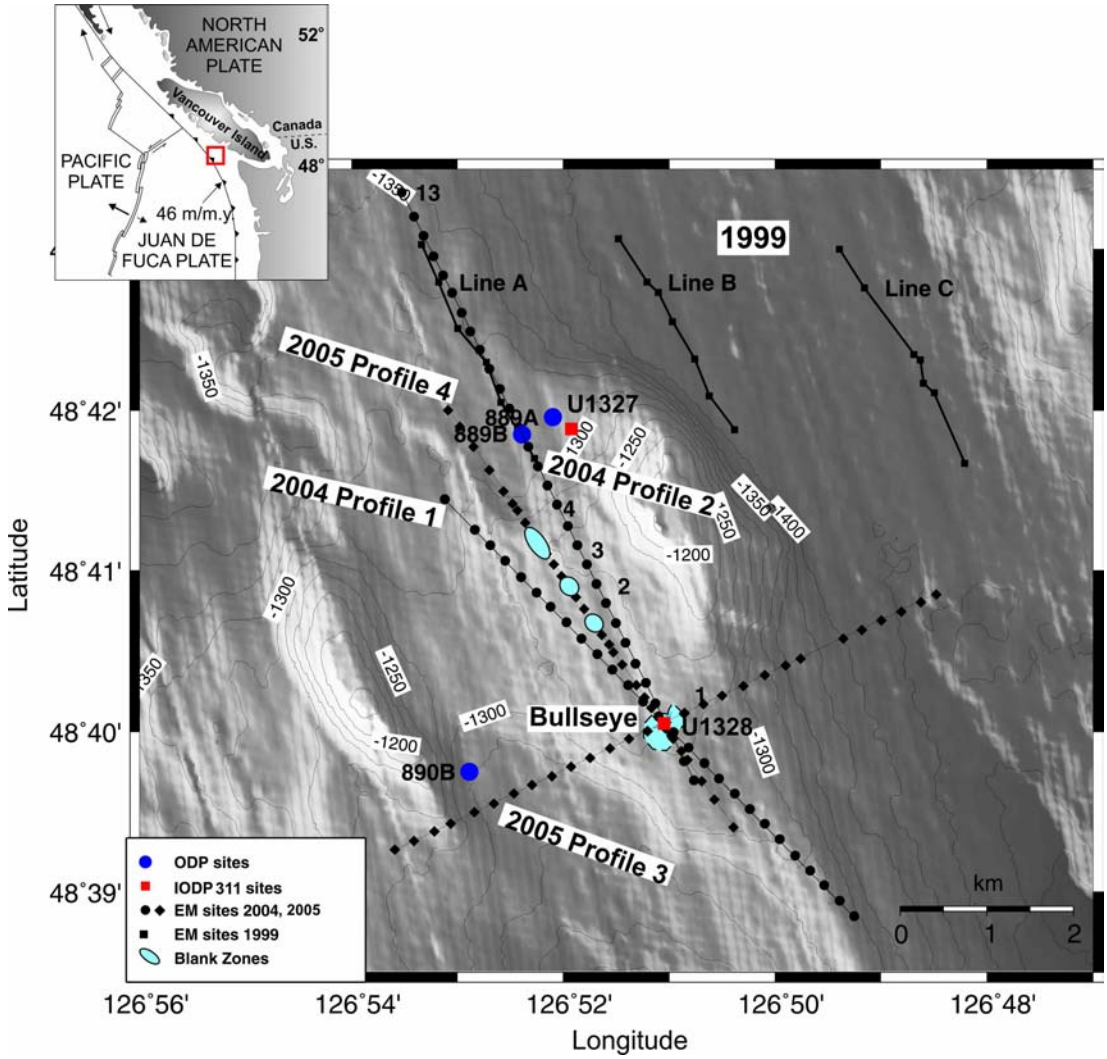

Figure 1: *Survey area on the Cascadia Margin in vicinity of ODP site 889. A series of seismic blank zones has been detected on a bathymetric bench in 1300m water depth between two topographic heights. BSRs have been identified in the entire area. Samples of gas hydrate were collected within the largest of the blank zones called 'Bullseye'. CSEM data along four profiles have been obtained across Bullseye and close to the other cold vents. Bullseye is also the location of IODP site U1328. Lines A, B, and C are the survey lines by Yuan and Edwards (2000).*

if gas hydrate is present (ρ_f: formation resistivity, ρ_w: seawater resistivity, Φ: porosity, $S_h=1-S_w$: gas hydrate saturation). Applying Archie's law requires estimates of the coefficients a, m and n which is described in e.g. Collett and Ladd (2000). Hydrate quantification also requires a reference no-hydrate-bearing data set. However, the additional hydrate concentration may be deduced by subtraction a background concentration from the data (Schwalenberg et al., 2005).

The University of Toronto has developed a bottom-towed transient electric dipole dipole system to sound the electrical resistivity distribution of the seafloor to a depth of several hundred meters. On the seafloor, the system consists of a transmitting dipole and two receiving dipoles (RX1, RX2) which are dragged in an inline configuration behind the transmitter (TX) (Figure 2). The two receivers are sensitive to different depth scales and provide a better resolution with depth. Typical transmitter receiver separations are between 150 and 400 m. The current source

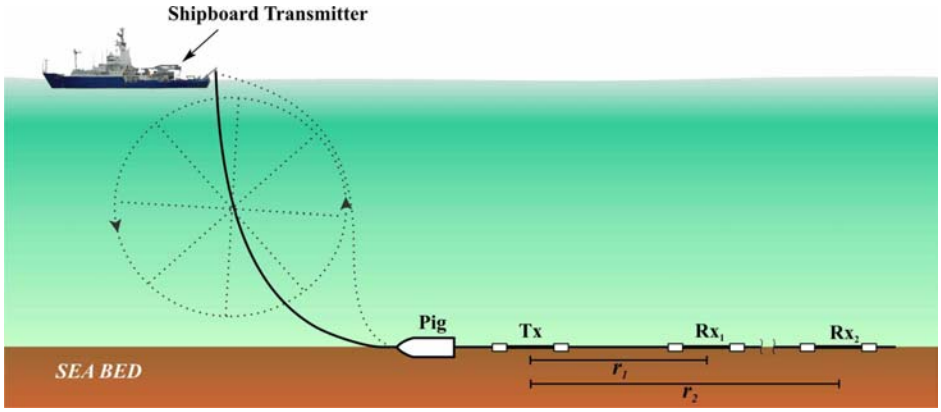

Figure 2: *Geometry of the inline dipole dipole system. On the seafloor the array consists of a transmitter dipole Tx followed by two receiver dipoles, Rx1 and Rx2 at distances r1 and r2. The pig, a heavy weight, is attached to the front of the array to keep it in contact with the sediments. The seafloor array is connected to the deep sea cable. A current signal is generated by a transmitter on board and send through the cable to the transmitter dipole on the seafloor. The cable follows the shape of a catenary (solid line). If pulled in, the cable appears to moves over an imaginary wheel below the ship (dotted line) (Schwalenberg et al., 2005).*

is located on the ship, has a maximum output of 9 kW, and follows any given reference signal. The system is operated in the time domain. For the chosen experimental set up, the signal has a square wave form and is sent through the coaxial cable to the transmitter dipole on the seafloor. On the seafloor, the electrical disturbance travels along two pathways to the receivers. One path is through the seawater and the other path is through the sediments. In shallow water, if the water depth is about or smaller than the transmitter receiver separation, a third path must
be considered, namely the one through the air which may mask the seafloor signal (Edwards, 2006). The signal propagating through the sediments arrives at the receiver first. The late time signal is mainly a function of the seawater conductivity and is generally eliminated from the analysis. Delay times and shapes of the signal sampled at the receiver depend on the resistivity structure of the seafloor and the transmitter receiver separation and may be analyzed similarly to seismic reflection data (Edwards, 2006).

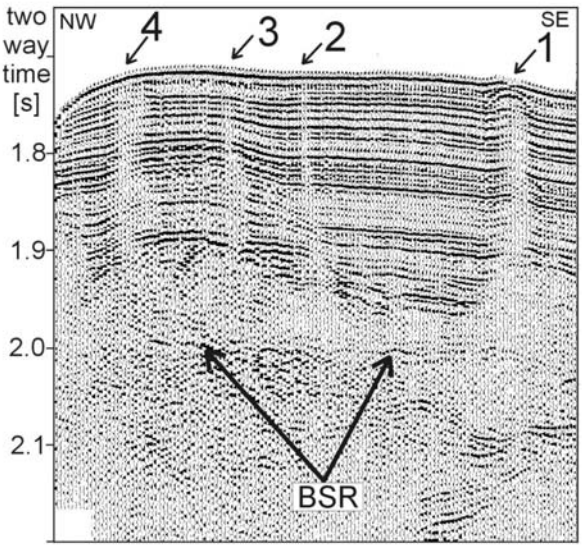

Figure 3 *Seismic section shows a BSR and four blank zones associated with cold vents (Riedel et al., 2002).*

Measurements are taken along profiles from site to site. The seafloor array stops during the data acquisition to avoid streaming potentials of the receiver electrodes due to movements in the seawater. Each receiver dipole is equipped with a self-contained electrical unit for data storage, signal synchronization, analog electronics and battery supply for up to 36h deployment time (see Schwalenberg et al., 2005 and 2006 for more detailed descriptions). Both, time domain (Scholl, open software 2006) and frequency domain software (Edwards, open software, 2005) exists to convert the data into one-dimensional models. However, it was generally possible to interpret the data with a single parameter - the resistivity of the lower halfspace. 3D modeling approaches are currently on the way using Druskin and Knizhnerman' s code (1994) to explain the highly anomalous data over the vents.

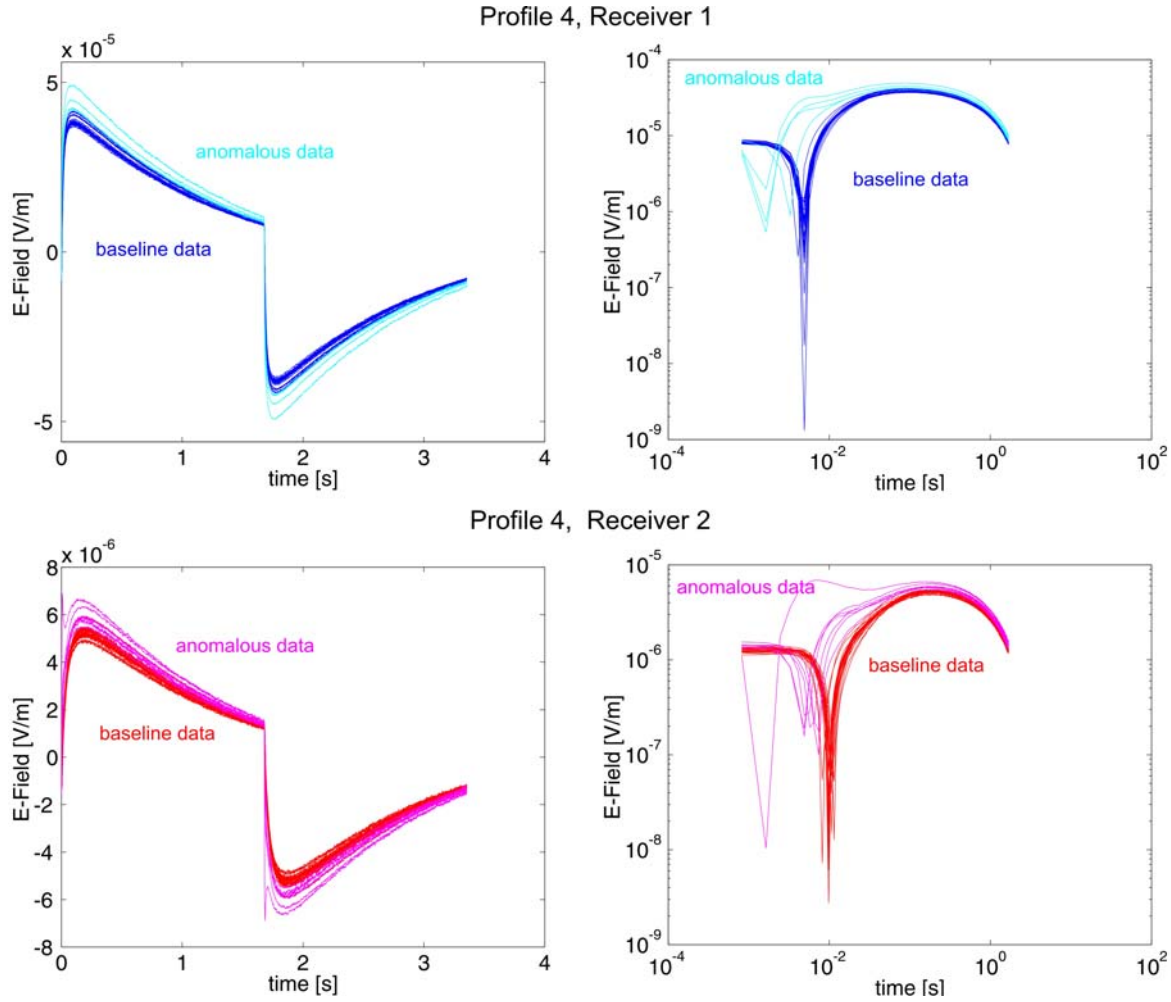

Figure 4: *Data along profile 4 as linear (left panels) and loglog plots (right panels) for receiver 1 (top, separation: 174m) and receiver 2 (bottom, separation 292m). The decay of the signal is caused by the low cut filter at the input of the receiver electronics. The anomalous data over the vents (cyan or magenta) have higher amplitudes and different signal shapes*.

CSEM Surveys

ODPSite 889

The first CSEM experiments on the Cascadia Margin using the Toronto system were conducted by Yuan and Edwards (2000) (also Yuan, 2003). They were designed to determine the electrical signature of the gas hydrate deposits in vicinity of ODP site 889 (Lines A, B, C in Figure 1). The analysis of the collected data resulted in uniform resistivities over areas with and without BSR signature. The BSR is an expression of the seismic impedance contrast between hydrate bearing sediments above and a layer of free gas below the base of the GHSZ (e.g. Hyndman and Davis, 1992). The BSR may disappear if the gas layer does not exist - without excluding the formation of gas hydrate within the GHSZ. Therefore the CSEM data suggest that gas hydrates are present in the survey area even where no BSR is visible (Yuan and Edwards, 2000).

Electrical resistivity logs of site 889 revealed increased resistivities between 1 and 2 Ωm. These values have been attributed to an increased hydrate concentration within the GHSZ. Hyndman et al., (2001) calculated gas hydrate concentrations from core data and showed values varying on average between 20 to 35% of the pore volume. Riedel et al. (2005) used logging data from ODP Leg 146 to re-evaluated the hydrate concentration and showed that the concentrations could be alternatively between 5 and 10%.

Gas hydrate concentrations were also calculated using Archie's law. The coefficients involved were determined by Hyndman et al. (1999) to a=1.4, m=1.76, and n=1 using core data from sites 888 and 889/890. Collett (2001) redefined these parameters to a=1, m=2.8, and n=1.9. All these values will be revised by the analyses of the observations made during the recent IODP transect, but these data are not available to the general public yet.

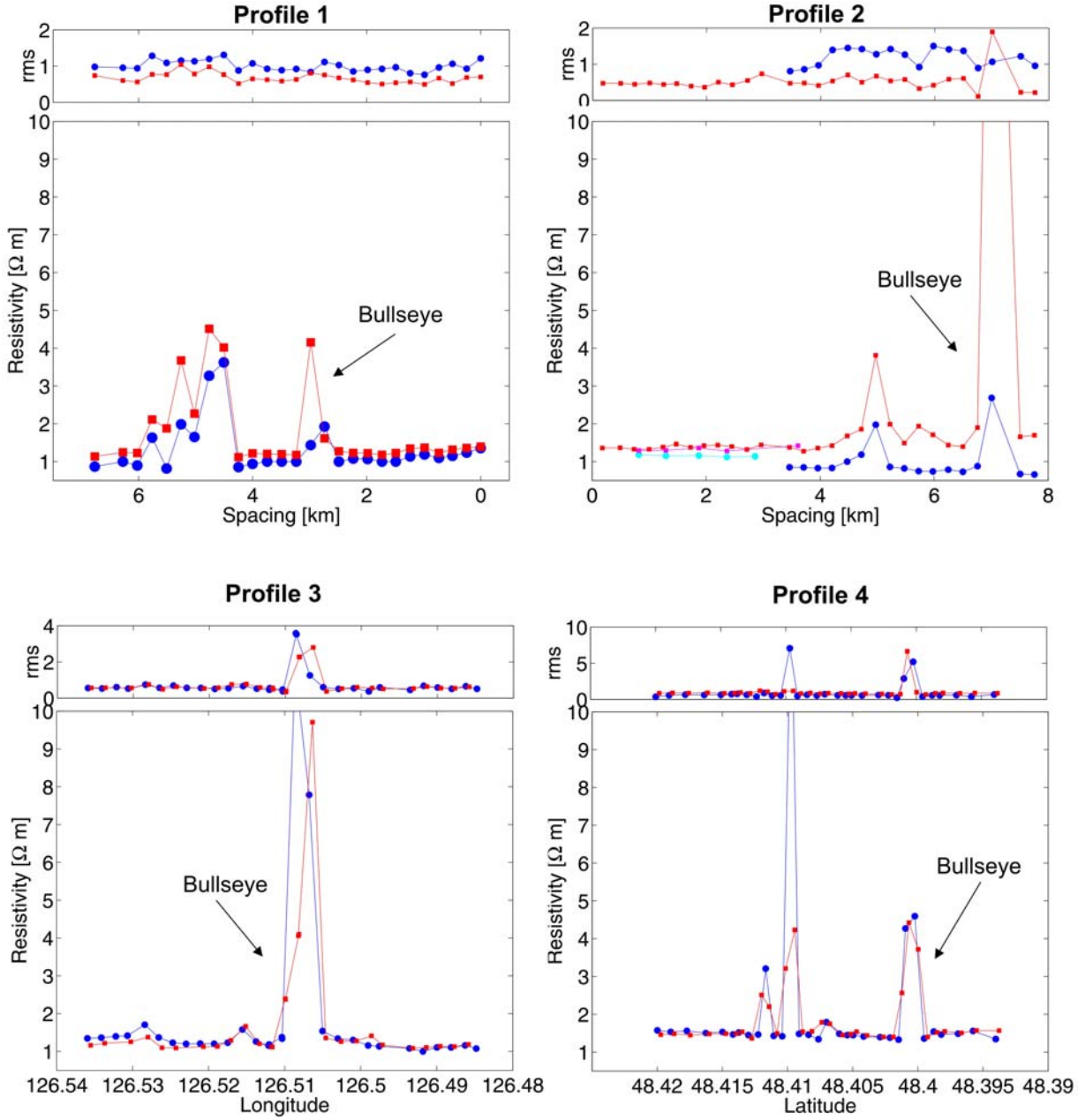

Figure 5: *Highly anomalous resistivities have been inverted over the vents along all four profiles. The resistivities are 4 times or more higher than the baseline resistivities which are surprisingly uniform. Small rms errors suggest the lower halfspace assumption is a good approximation outside the vents. Within the vents the models have to be refined, but clearly indicate the existence of large amounts of very resistive material. The top right panel also shows the results of Yuan and Edwards (2000) along Line A.*

Vent Field

The vent field is characterized by at least 4 distinct seismic blank zones underlain by a BSR seen in different seismic data sets (Figure 3, Riedel at al., 2002). Whether the origin of the blank zones is due to free gas or gas hydrate or a combination of both has been strongly debated. Discussions of the vents and Bullseye in particular can be found in Wood et al. (2002), Zühlsdorff and Spiess (2004), Riedel at al., (2002, 2006).

In the summers of 2004 and 2005, CSEM data have been collected on Canadian Coast Guard Ship J.P. Tully. Four profiles have been completed, each about 7 km long with a site spacing of 250m and 150m, respectively. The transmitted current is a square wave switching between plus and minus 10 A with a period of 6.7 s or 3.4 s, respectively. The data collected are sets of stacked and raw time series of the receiver transients (Figure 4).

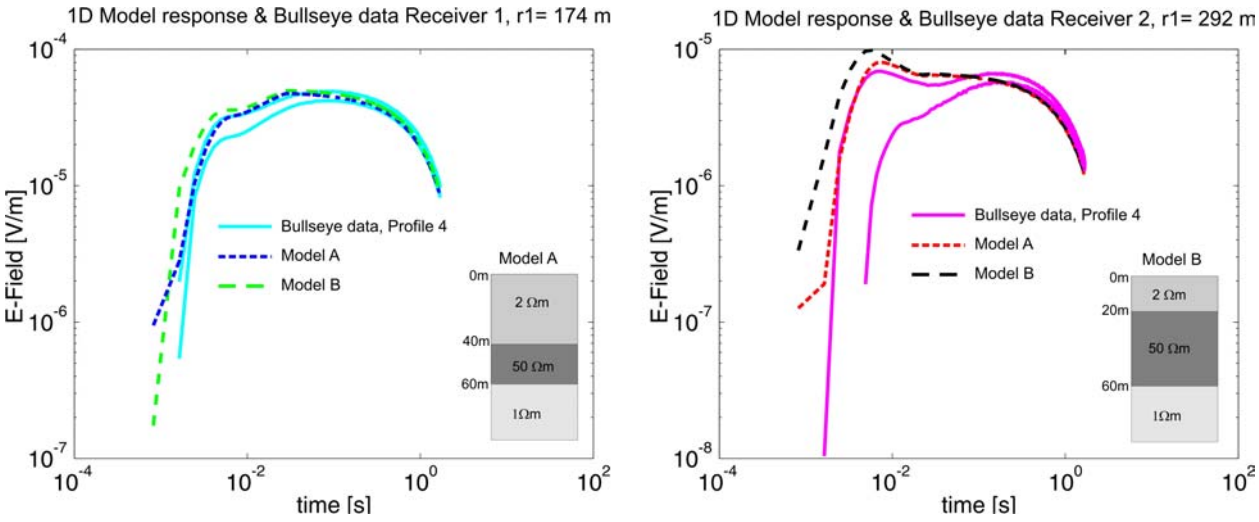

Figure 6: *1D layered modeling has been started to fit the anomalous data over bullseye. Displayed are the results for two models A and B compared with bullseye data from profile 4. Model A shows a reasonable fit to the data from one site. However, this is work in progress and will be applied to cross-check 1D inversion and 3D modeling results.*

Results

At first, the data from profiles 1 to 4 have been inverted to lower halfspace resistivities using Edwards (open software, 2005). All four profiles in Figure 5 show highly anomalous resistivities over the vents and remarkably uniform values otherwise. The resistivities rise up to values about 5 Ωm or even higher over baseline resistivities which vary between 1 and 1.5 Ωm from profile to profile. Small root mean square errors demonstrate at least the baseline data can be explained by a single parameter. This is not true over the vents. Being clearly anomalous, the modeled resistivity values above 10 Ωm are presumably artifacts and the results of a false a priori assumption.

In a next step, 1D layered modeling has been employed to better fit the anomalous data over the vents. In Figure 6, data at Bullseye from profile 4 are compared with the 1D impulse responses of models A and B convolved with the system response. Model A partly explains the data reasonably well, but

Also multi-layered 1D inversion is on the way. Figure 7 shows a preliminary section of stitched 1D results along profile 4. The data from both receiver dipoles were used in a time domain joint smooth model inversion. Again, the results for the vent sites differ significantly from those for the baseline data sets, which are mutually similar. The average background or baseline model has essentially three layers: a very conductive upper layer, 0.9Ωm 25m thick, followed by a more resistive layer, 1.7Ωm ~75m thick, terminated by a more conductive

halfspace around 1 Ωm which is poorly resolved. The models associated with the vent sites show extreme resistivity structures and strong lateral changes. This indicates that – despite of the moderate misfits at most of these sites – a 1D model may not fit the data and the data are distorted by a multidimensional structure associated with the vents.
However, the vents are clearly 3D targets and the process of 3D forward modeling has been started using the 3D finite difference code by Druskin and Knizhnerman (1994).

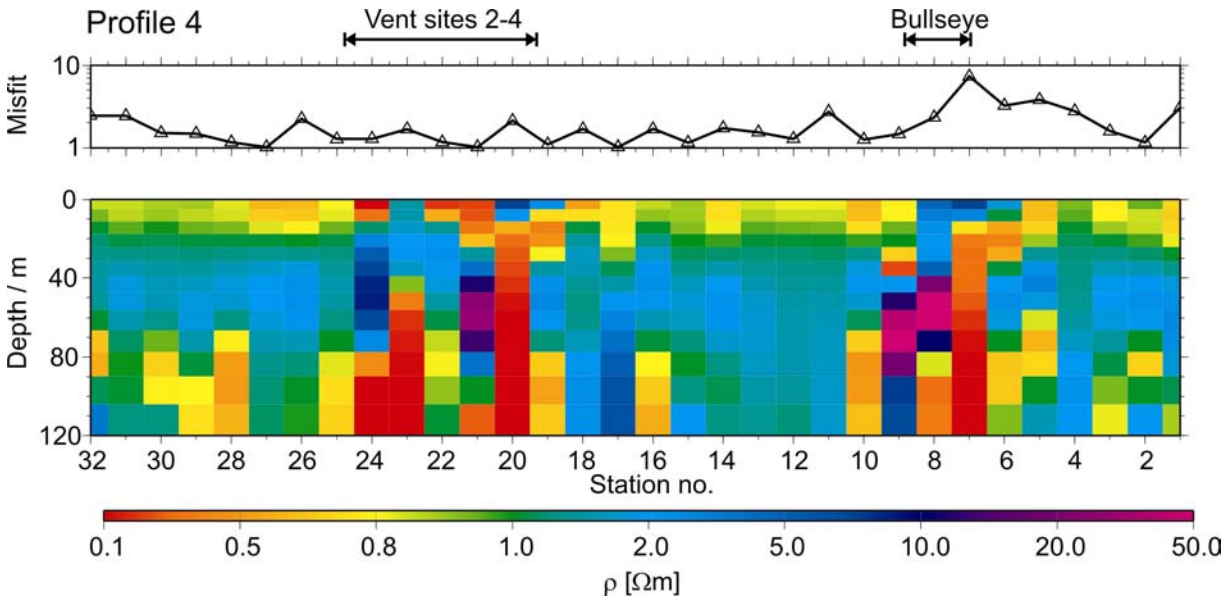

Figure 7: *Stitched results of 1D joint inversions for the data set recorded along profile 4. The displayed misfit is an error weighted RMS. The models obtained at stations close to the vent sites ("Bullseye" and "Vent sites 2-4") show strong lateral and vertical variations, indicating distortions by multidimensional structures.*

Discussion

Very large amounts of resistive material are required to explain the highly anomalous resistivities observed over the cold vents. Possible candidates are a higher gas hydrate concentration within the vents, free gas, or a combination of both. Free gas alone or in a predominantly concentration is very unlikely. This would contradict observations made by e.g. Willoughby et al., (2006) who observed higher shear moduli derived from compliance data at Bullseye. The presence of free gas within the GHSZ would also result in the formation of hydrate until the pore water is depleted. A higher hydrate concentration may explain the observed anomalies, probably combined with sufficient free gas to scatter seismic reflection signals. Further, the presence of the BSR below the vents in Figure 3 suggests that gas hydrate is present in the entire area.
For a first rough estimate we may calculate the additional hydrate concentration from Archie's modified law by subtraction a background concentration from the "total" observed concentration. The background concentration is derived from the baseline resistivities as the total concentration is derived from the inverted resistivity profile. Figure 8 shows the resistivity profile and the additional hydrate concentration derived from profile 1 (see also Schwalenberg et al., 2005). Archie's law parameter were set to a=1, m=2.8, and n=1.9 (Collett, 2000, Riedel et al., 2005), and an average porosity of 60% (e.g. Hyndman et al., 1999) was employed in the calculation. This approach results in an additional hydrate concentration of more than 50% maximum and about 25% on average. Taken into account a solid to gas ratio of 1:164 the related methane gas volume at STP would be 0.62 billion m^3 for a cylindrical volume with a diameter of 400m and a depth of 200m (Schwalenberg et al., 2005).

Recent drilling results at IODP site U1238 at Bullseye suggest, that the hydrate distribution is heterogeneous within the logs and from drill hole to drill hole. The highest gas hydrate concentration has been found in an interval of 0 to 40 mbsf in the centre of a seismically imaged hydrate cap (M. Riedel, personal communication). Based on the seismic data, the hydrate would be expected to be progressively deep with radial distance from the centre of the Bullseye vent. These information will be incorporated in the ongoing modeling process. However, CSEM data and logging data are sensitive on a different scale. The former are averaging over a larger volume while the latter provide detailed information of a comparable small volume.

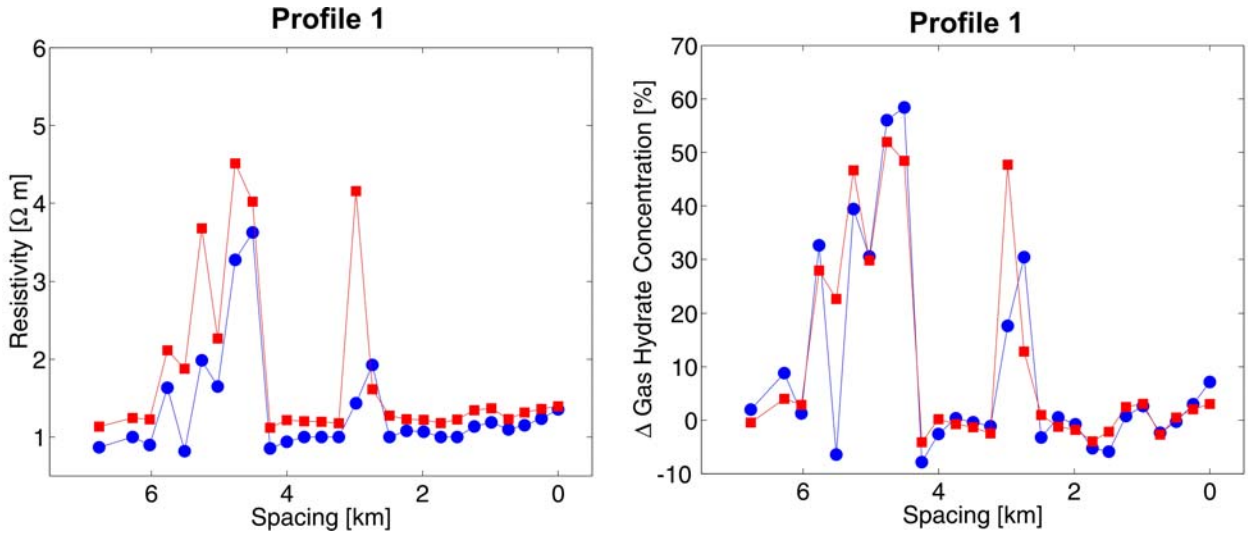

Figure 8: *The left panel shows again the resistivity profile 1. Assuming the anomalous resistivities are caused by a locally higher gas hydrate concentration within the vents, we may estimate the additional gas hydrate concentration using Archie's modified law. Therefore, the regional gas hydrate concentration derived from baseline resistivties has been subtracted from the "total" observed concentration (right panel).*

Outlook

The Toronto design is currently updated towards a modular multi-receiver system with a fibre optic link between the data acquisition box towed behind the transmitter and the receiver units. Ship time is scheduled in Cascadia in summer 2006 for instrument tests and gas hydrate surveying. Borehole to borehole measurements are being considered to sound the sediment section of the GHSZ. Software developments aim at multi-dimensional time - and frequency domain solutions.

Acknowledgements

We thank the captains and crews of C.C.G.S. John P. Tully for excellent support. The research is funded by grants to RNE from the Natural Science and Engineering Research Council of Canada. Ship time was provided by the Geological Survey of Canada. KS was holding a Fellowship from the German Research Foundation and ECW holds a NSERC Fellowship. The Institute of Geophysics and Meteorology, University of Cologne, Germany kindly allowed us to use their 3D code.

Literature

Archie, G.E. [1942] The electrical resistivity log as an aid in determining some reservoir characteristics. Journal of Petroleum Technology, 5, 1-8.

Collett, T.S. and Ladd J. [2000] Detection of gas hydrate with downhole logs and assessment of gas hydrate concentrations (saturations) and gas volumes on the Blake Ridge with electrical resistivity log data, in Paull, C. K., Matsumoto R., Wallace, P. J., and Dillon, W. P. (eds.), Proceedings of the Ocean Drilling Program, Scientific Results, Vol. 164, 179 – 191.

Collett, T.S., [2001] A review of well-log analysis techniques used to assess gas-hydrate-bearing reservoirs, in: Natural gas hydrates, Occurrence, Distribution and Detection, (ed. C.K. Paull and W.P. Dillon), Geophysical Monograph Series No. 124, pp. 189 – 210, American Geophysical Union (AGU).

Druskin, V., and Knizhnerman, L. [1994] Spectral approach to solving three dimensional Maxwell's diffusion equations in the time and frequency domains: Radio Science, 29, No. 4, 937–953.

Edwards, R.N. [1997] On the resource evaluation of marine gas hydrate deposits using sea-floor transient electric dipole-dipole method. Geophysics. Vol.62, No.1, 63-74.

Edwards R.N. [2006] Marine Controlled Source Electromagnetics: Principles, Methodologies, Future Commercial Applications', Invited Review Paper, *Surveys in Geophysics*, 26, 675-700.

Expedition 311 Scientists, 2005. Cascadia margin gas hydrates. *IODP Prel. Rept.,* 311. doi:10:2204/ iodp.pr.311.2005

Hyndman, R.D., and Davis, E.E. [1992] A mechanism for the formation of methane gas hydrate and seafloor bottom-simulating reflectors by vertical fluid expulsion: Journal of Geophysical Research, v. 97, p. 7125-7041.

Hyndman, R.D., Yuan, T., Moran, K. [1999] The concentration of deep sea gas hydrates from downhole electrical resistivity logs and laboratory data. Earth and Planetary Science Letters 172, 167-177.

Hyndman, R.D., G.D. Spence, R. Chapman, M. Riedel, and R.N. Edwards [2001] Geophysical studies of marine gas hydrate in northern Cascadia. Natural Gas hydrates: Occurrence, Distribution, and Detection, AGU Monograph, Vol. 124, 273-295.

Riedel, M., Spence, G.D., Chapman, N.R., Hyndman, R.D. [2002] Seismic investigations of a vent field associated with gas hydrates, offshore Vancouver Island. Journal of Geophysical Research 107 (B9), doi:10/1029/2001JB000269.

Riedel, M., Collett, T.S., and Hyndman, R.D, [2005] Gas hydrate concentration estimates from chlorinity, electrical resistivity and seismic velocity. Geological Survey of Canada, Open File No. 4934.

Riedel, M., Novosel, I., Spence, G.D., Hyndman, R.D , Chapman, N.R., Solem R.C., and Lewis, T. [2006] Geophysical and geochemical signatures associated with gas hydrate related venting at the northern Cascadia Margin. Review paper, GSA Bulletin, Jan/Feb 2006, Vol. 118, No. 1/2, 23-38, doi: 10.1130/B25720.1.

Schwalenberg K., Edwards R.N, Willoughby E.C, Yuan J, Cairns G, and Diaz-Naveas J [2004] Marine controlled source electromagnetic experiment to evaluate gas hydrates off the coastlines of North and South America. Proceedings, 4th MARELEC Conference, London, UK 17-18 March 2004.

Schwalenberg K., E.C. Willoughby, R. Mir, and R.N. Edwards [2005] Marine gas hydrate electromagnetic signatures in Cascadia and their correlation with seismic blank zones. First Break, Vol. 23, 57-63.

Schwalenberg, K., Edwards, R.N., Cairns, G.M. and Willoughby, E.C. [2006] A controlled source electromagnetic experiment to assess gas hydrates in marine sediments offshore Chile. Submitted to J. Geophys. Res.

Spence, G.D., R.D. Hyndman, N.R. Chapman, M. Riedel, N. Edwards, and J. Yuan [2000] Cascadia margin, northeast Pacific Ocean: Hydrate distribution from geophysical observations. Natural Gas Hydrate in Oceanic and Permafrost Environments, Kluwer Acad. Publ., 183-198.

Willoughby E.C and Edwards R.N. [2000] Shear Velocities in Cascadia from Seafloor Compliance Measurements. Geophysical Research Letters, 27, 1021-1024.

Willoughby, E.C., K. Latychev, R.N. Edwards, K. Schwalenberg and R.D. Hyndman *[*(2006] Seafloor Compliance Imaging of Marine Gas Hydrate Deposits and Cold Vent Structures, *J. Geophys. Res (submitted)*

Wood, W.T., Gettrust, J.F., Chapman, N.R., Spence, G.D., and Hyndman R.D. [2002] Decreased stability of methane hydrate in marine sediments owing to phase boundary roughness. Nature Vol. 420, 656-660.

Yuan J. and R.N. Edwards [2000] The assessment of marine gas hydrate through electrical remote

sounding: Hydrate without a BSR? *Geophysical Research Letters*, 27, 2397-2400.

Yuan, J. [2003] Electromagnetic assessment of offshore methane hydrate deposits on the Northern Cascadia Margin, PhD Thesis, *Geophysics Laboratory, University of Toronto*

Zühlsdorff, L., and V. Spiess, [2004] Three-dimensional seismic characterization of a venting site reveals compelling indications of natural hydraulic fracturing: Geology, Vol 32, No. 2, 101-104.